Quarkonia production in (ultra-)peripheral PbPb collisions at LHCb

Xiaolin Wang on behalf of the LHCb collaboration
xiaolin.wang@cern.ch

South China Normal University, Guangzhou, China

Presented at DIS2022: XXIX International Workshop on Deep-Inelastic Scattering and Related Subjects, Santiago de Compostela, Spain, May 2-6 2022.

Abstract: The cross-sections of coherent J/ψ and $\psi(2S)$ production in ultra-peripheral PbPb collisions at a nucleon-nucleon centre-of-mass energy of 5.02 TeV are measured using a data sample collected in 2018 at LHCb, and the differential cross-sections are measured separately as a function of transverse momentum and rapidity. The photo-production of J/ψ mesons at low transverse momentum is studied in peripheral PbPb collisions, J/ψ candidates are reconstructed through the prompt decay into $\mu^+\mu^-$ in the rapidity region of $2.0 < y < 4.5$. These results significantly improve previous measurements and are compared to the latest theoretical predictions.

1. Introduction

The LHCb detector is a single-arm forward spectrometer covering the unique pseudorapidity range $2 < \eta < 5$ [1, 2], which could provide precise vertex reconstruction, high particle momentum resolution and excellent particle identification ability. The quarkonia production in (ultra-)peripheral collisions is sensitive to the gluon parton distribution function in nuclear at small-x, and coherent photo-production would provide an excellent laboratory to study the nuclear shadowing effects and the initial state of quark-gluon plasma with small-x at the LHC [3].

2. Study of charmonium production in ultra-peripheral PbPb collisions at LHCb [4]

Ultra-peripheral collisions(UPCs) occur when the distance between the center of two nuclei is larger than the sum of their radii [5]. The two ions interact via their cloud of semi-real photons and photon-nuclear interactions dominate. The basic process is electromagnetic and strong interactions are suppressed. In UPCs, J/ψ and $\psi(2S)$ mesons are produced from the colourless exchange of a photon from one nucleus and a pomeron from the other. Coherent production occurs when the photon interacts with a pomeron emitted by the entire nucleus, which is the process we are going to study.

The charmonium candidates are reconstructed through the $J/\psi \to \mu^+\mu^-$ and $\psi(2S) \to \mu^+\mu^-$ decay channels, using 2018 PbPb data sample corresponding to an integrated luminosity of $228 \pm 10\,\mu\text{b}^{-1}$. The signal yields are extracted in two steps. First, a fit on the dimuon invariant mass spectrum is needed to estimate the charmonium and non-resonant background yields within the J/ψ and $\psi(2S)$ mass windows, respectively. The mass distribution along with the dimuon mass fit is shown in Fig 1. Then fits to J/ψ or $\psi(2S)$ $\ln(p_{\text{T}}^{*2})$ distributions are performed to

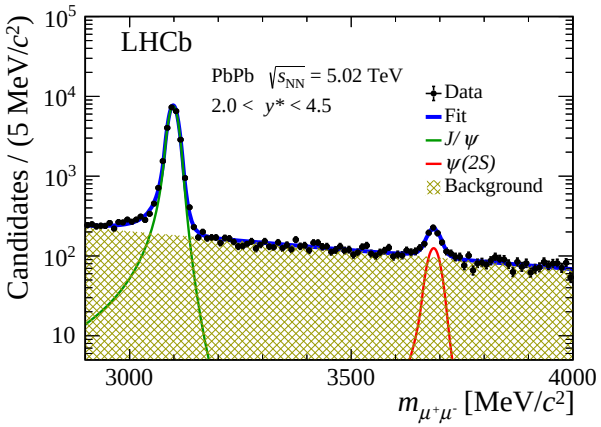

Fig. 1: Dimuon mass distribution fit for signal candidates in the rapidity range $2.0 < y^* < 4.5$.

determine the coherent production events from the yields in corresponding mass windows, where the starred notation indicates that the observable is defined in the nucleus-nucleus centre-of-mass frame. Figure 2 shows the fits to the $\ln(p_{\mathrm{T}}^{*2})$ distributions of selected J/ψ and $\psi(2S)$ candidates within rapidity interval $2.0 < y^* < 4.5$. The shapes of coherent, incoherent and $\psi(2S)$ feed-down components are taken from simulation, and the shape of non-resonant background is taken from the mass window, $3.2 < m_{\mu^+\mu^-} < 3.6\,\mathrm{GeV}/c^2$, where there is no signal component. The yields of the non-resonant background are determined as the integral of the non-resonant component from the dimuon mass fit in the J/ψ and $\psi(2S)$ mass windows.

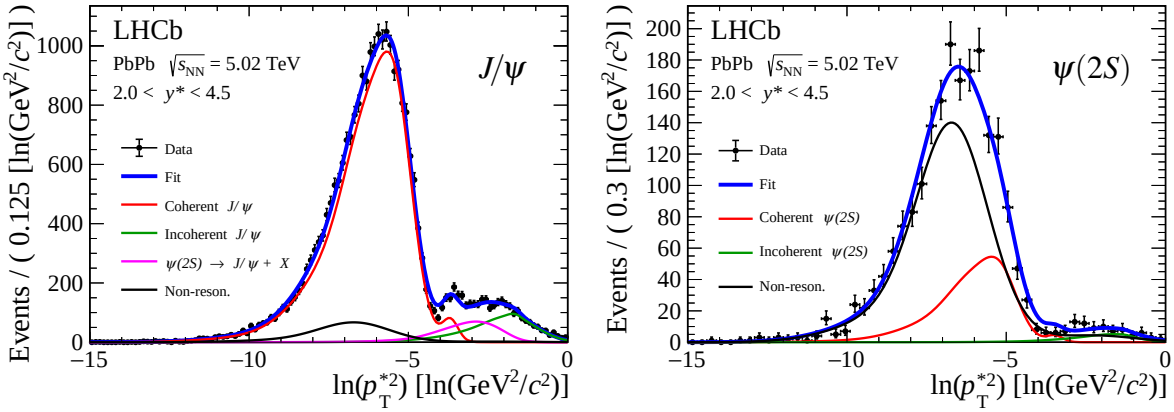

Fig. 2: The $\ln(p_{\mathrm{T}}^{*2})$ distribution fit of dimuon candidates in the $2.0 < y^* < 4.5$ range for (left) J/ψ candidates and (right) $\psi(2S)$ candidates.

The results of coherent J/ψ and $\psi(2S)$ differential cross-sections as a function of rapidity and their ratio are calculated in five rapidity bins and shown in Fig. 3. The differential production cross-sections as a function of transverse momentum are also measured separately and shown in Fig. 4. We also compared the results between experimental measurements and theoretical predictions [6–15]. Also, there are two previous results of coherent J/ψ production in PbPb UPCs by the LHCb [16] and ALICE [17] experiments. Compared with above measurements, we see this new result is slightly larger than the previous LHCb result by around 2σ and more compatible with the ALICE measurement.

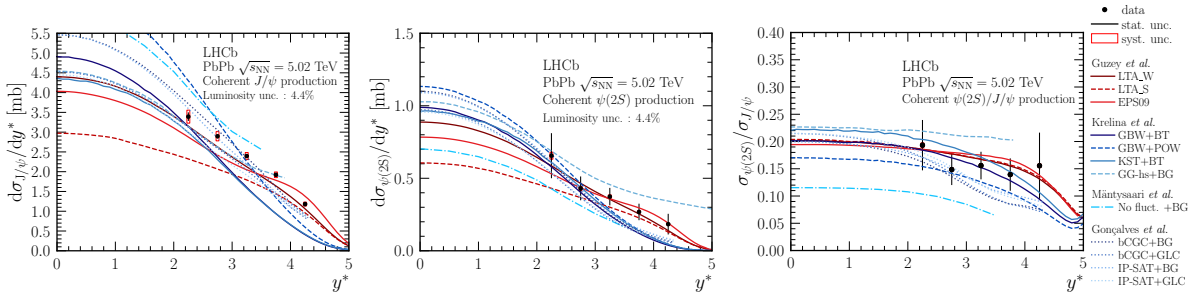

Fig. 3: Differential cross-section as a function y^* for coherent J/ψ , $\psi(2S)$ production and the ratio of coherent $\psi(2S)$ to J/ψ production, compared to theoretical predictions. These models are grouped as (red lines) perturbative-QCD calculations and (blue lines) colour-glass-condensate models.

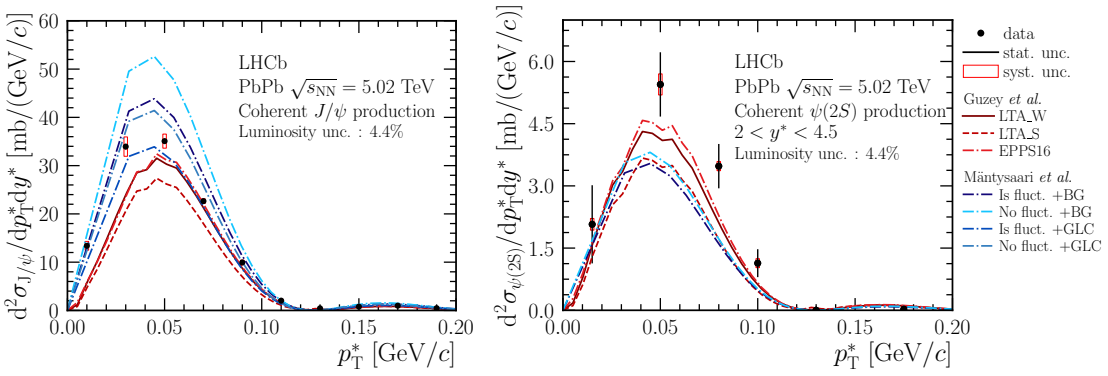

Fig. 4: Differential cross-section as a function of p_T^* within the rapidity range $2 < y^* < 4.5$ for coherent (left) J/ψ and (right) $\psi(2S)$ production compared to theoretical predictions.

3. Study of J/ψ photo-production in PbPb peripheral collisions at $\sqrt{s_{NN}} = 5$ TeV [18]

In peripheral collisions, the impact parameter b is less than the sum of radii, so there is not only photo-nuclear interaction but also hadronic interaction. The photo-produced J/ψ is expected to

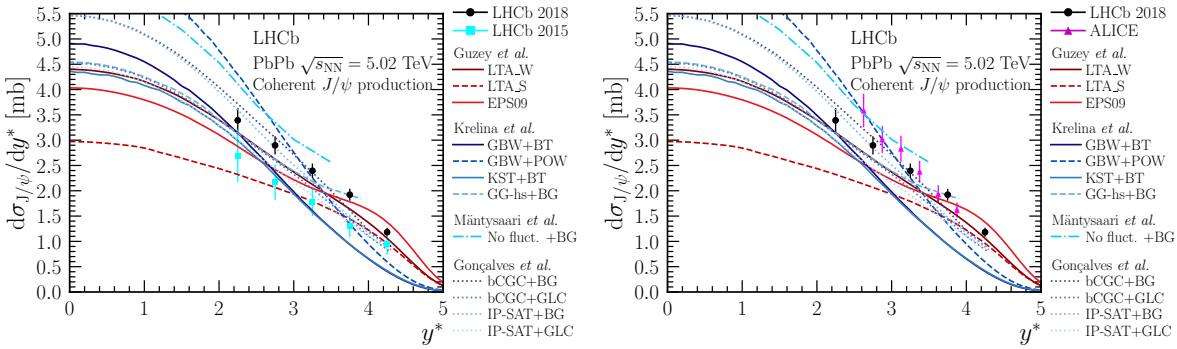

Fig. 5: Differential cross-sections as a function of rapidity for coherent J/ψ production compared to the previous measurements by the LHCb [16] and ALICE [17]. The measurements are shown as dots and squares, where the uncertainties represent total uncertainties respectively. Then both results are compared to theoretical predictions [6–15].

have a very low transverse momentum of less than 300 MeV/c, whereas the hadronic produced J/ψ typically have transverse momentum of about 1-2 GeV/c. Thanks to the high precision of the LHCb experiment, the very low p_{T} region can be explored and the number of photo-produced J/ψ could be extracted, as shown in Fig. 6.

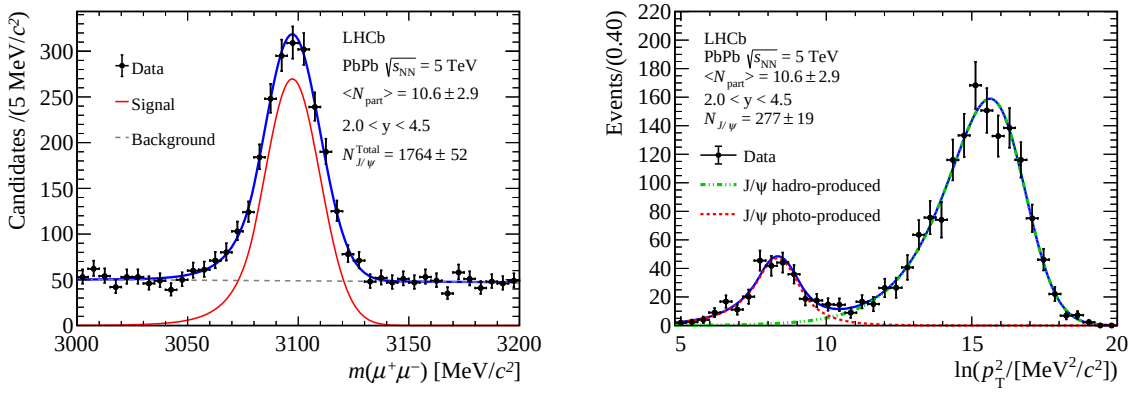

Fig. 6: The $\ln(p_{\mathrm{T}}^{*2})$ distribution of dimuon candidates in the $2.0 < y^* < 4.5$ range for (left) J/ψ candidates and (right) $\psi(2S)$ candidates. The data are overlaid with the result of the fit.

The differential photo-production yields of J/ψ versus the rapidity, the number of participants in the collision, and the double-differential J/ψ photo-production yields versus transverse momentum as shown in Fig. 7, and are compared to theoretical calculations. One scenario does not consider the destructive effect due to the overlap between the two nuclei, whereas the other takes it into account. The two theoretical curves do not show a significant difference because the collisions are peripheral. This nuclear overlapping effect is expected to increase at more central collisions. The trend between J/ψ photo-production measurements and theoretical predictions are consistent in general.

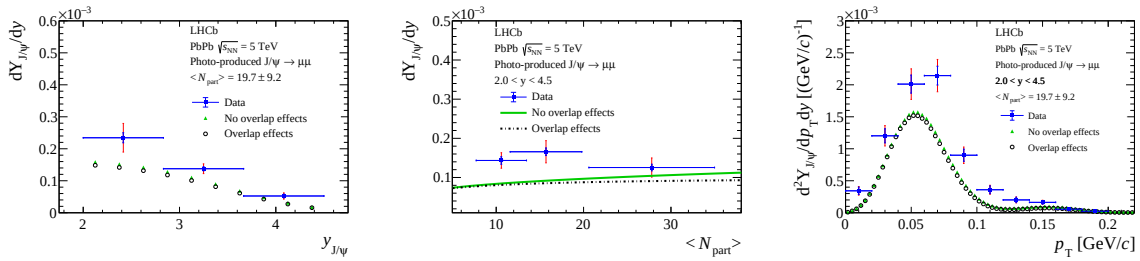

Fig. 7: The results of the differential photo-production yields of J/ψ versus the rapidity, the number of participants in the collision and the double-differential J/ψ photo-production yields versus transverse momentum.

4. Conclusion

The cross-sections of coherent J/ψ, ψ(2S) production, and their ratio in UPCs are measured using the 2018 PbPb dataset. It is the first coherent $\psi(2S)$ measurement in forward rapidity region for UPC at LHC and the first time to measure the coherent J/ψ and $\psi(2S)$ production cross-sections versus p_{T} distribution in PbPb UPCs. The measurement of photo-produced J/ψ mesons in peripheral PbPb collisions using the 2018 dataset is the first result using PbPb hadronic

collisions data by the LHCb and also the most precise coherent photoproduced J/ψ measurement to date.

References

1. LHCb Collaboration, A. A. Alves Jr. *et al.*, *The LHCb detector at the LHC*, JINST **3** (2008) S08005.
2. LHCb Collaboration, R. Aaij *et al.*, *LHCb detector performance*, Int. J. Mod. Phys. **A30** (2015) 1530022, arXiv:1412.6352.
3. S. P. Jones, A. D. Martin, M. G. Ryskin, and T. Teubner, *Exclusive J/ψ and Υ photoproduction and the low x gluon*, J. Phys. **G43** (2016) 035002, arXiv:1507.06942.
4. LHCb collaboration, *Study of coherent charmonium production in ultra-peripheral lead-lead collisions*, arXiv:2206.08221.
5. C. A. Bertulani, S. R. Klein, and J. Nystrand, *Physics of ultra-peripheral nuclear collisions*, Ann. Rev. Nucl. Part. Sci. **55** (2005) 271, arXiv:nucl-ex/0502005.
6. V. Guzey, E. Kryshen, and M. Zhalov, *Coherent photoproduction of vector mesons in ultraperipheral heavy ion collisions: Update for run2 at the CERN Large Hadron Collider*, Phys. Rev. **C93** (2016) 055206, arXiv:1602.01456.
7. V. Guzey, M. Strikman, and M. Zhalov, *Accessing transverse nucleon and gluon distributions in heavy nuclei using coherent vector meson photoproduction at high energies in ion ultraperipheral collisions*, Phys. Rev. **C95** (2017) 025204, arXiv:1611.05471.
8. V. P. Gonçalves and M. V. T. Machado, *Vector meson production in coherent hadronic interactions: an update on predictions for RHIC and LHC*, Phys. Rev. **C84** (2011) 011902, arXiv:1106.3036.
9. J. Cepila, J. G. Contreras, and M. Krelina, *Coherent and incoherent* J/ψ *photonuclear production in an energy-dependent hot-spot model*, Phys. Rev. **C97** (2018) 024901, arXiv:1711.01855.
10. B. Z. Kopeliovich, M. Krelina, J. Nemchik, and I. K. Potashnikova, *Heavy quarkonium production in ultraperipheral nuclear collisions*, arXiv:2008.05116.
11. V. P. Gonçalves *et al.*, *Color dipole predictions for the exclusive vector meson photoproduction in pp, p*Pb*, and* PbPb *collisions at run2 LHC energies*, Phys. Rev. **D96** (2017) 094027, arXiv:1710.10070.
12. V. P. Gonçalves and M. V. T. Machado, *The QCD pomeron in ultraperipheral heavy ion collisions: IV. Photonuclear production of vector mesons*, Eur. Phys. J. **C40** (2005) 519, arXiv:hep-ph/0501099.
13. H. Kowalski, L. Motyka, and G. Watt, *Exclusive diffractive processes at HERA within the dipole picture*, Phys. Rev. **D74** (2006) 074016, arXiv:hep-ph/0606272.
14. H. Mäntysaari and B. Schenke, *Probing subnucleon scale fluctuations in ultraperipheral heavy ion collisions*, Phys. Lett. **B772** (2017) 832, arXiv:1703.09256.
15. T. Lappi and H. Mäntysaari, *Diffractive vector meson production in ultraperipheral heavy ion collisions from the color glass condensate*, PoS **DIS2014** (2014) 069, arXiv:1406.2877.
16. LHCb collaboration, R. Aaij *et al.*, *Study of coherent J/ψ production in lead-lead collisions at $\sqrt{s_{NN}} = 5TeV$*, arXiv:2107.03223.
17. ALICE collaboration, S. Acharya *et al.*, *Coherent J/ψ photoproduction at forward rapidity in ultra-peripheral Pb-Pb collisions at* $\sqrt{s_{\rm NN}} = 5.02$ *TeV*, Phys. Lett. **B798** (2019) 134926, arXiv:1904.06272.
18. LHCb collaboration, R. Aaij *et al.*, *J/ψ photoproduction in Pb-Pb peripheral collisions at $\sqrt{s_{NN}}$= 5 TeV*, Phys. Rev. C **105** (2022) L032201, arXiv:2108.02681.